Thieme

New Phenylethanoid Glycosides from *Cistanche phelypaea* and Their Activity as Inhibitors of Monoacylglycerol Lipase (MAGL)

Authors
Khadidja Aya Beladjila[1], Djemaa Berrehal[1], Nunziatina De Tommasi[2], Carlotta Granchi[3], Giulia Bononi[3], Alessandra Braca[3,4], Marinella De Leo[3,4]

Affiliations
1 Laboratoire d'Obtention des Substances Thérapeutiques (LOST), Département de Chimie, Université des Frères Mentouri-Constantine, Constantine, Algeria
2 Dipartimento di Farmacia, Università di Salerno, Fisciano, Italy
3 Dipartimento di Farmacia, Università di Pisa, Italy
4 Centro Interdipartimentale di Ricerca "Nutraceutica e Alimentazione per la Salute", Università di Pisa, Italy

Key words
Cistanche phelypaea, Orobanchaceae, phenylethanoid glycosides, cancer, monoacylglycerol lipase, lactate dehydrogenase

received October 30, 2017
revised December 21, 2017
accepted December 27, 2017

Bibliography
DOI https://doi.org/10.1055/s-0044-100187
Published online January 10, 2018 | Planta Med 2018; 84: 710–715 © Georg Thieme Verlag KG Stuttgart · New York | ISSN 0032-0943

Correspondence
Prof. Alessandra Braca
Dipartimento di Farmacia, Università di Pisa
Via Bonanno 33, 56126 Pisa, Italy
Phone: + 39 05 02 21 96 88, Fax: + 39 05 02 22 06 80
alessandra.braca@unipi.it

Supporting information available online at http://www.thieme-connect.de/products

ABSTRACT

Four new phenylethanoid glycosides (**1**–**4**), 1-*β*-*p*-hydroxyphenyl-ethyl-2-*O*-acetyl-3,6-di-*α*-L-rhamnopyranosyl-*β*-D-glucopyranoside (**1**), 1-*β*-*p*-hydroxyphenyl-ethyl-3,6-*O*-di-*α*-L-rhamnopyranosyl-*β*-D-glucopyranoside (**2**), 1-*β*-*p*-hydroxyphenyl-ethyl-2-*O*-acetyl-3,6-di-*α*-L-rhamnopyranosyl-4-*p*-coumaroyl-*β*-D-glucopyranoside (**3**), and 1-*β*-*p*-hydroxyphenyl-ethyl-3,6-di-*α*-L-rhamnopyranosyl-4-*p*-coumaroyl-*β*-D-glucopyranoside (**4**), together with three known compounds, were isolated from the *n*-butanol extract of *Cistanche phelypaea* aerial parts. The structural characterization of all compounds was performed by spectroscopic analyses, including 1D and 2D NMR, and HRESIMS experiments. The isolated compounds were assayed for their inhibitory activity on two enzymes involved in the peculiar glycolytic or lipidic metabolism of cancer cells, human lactate dehydrogenase (LDH), and monoacylglycerol lipase (MAGL), respectively. All the compounds showed negligible activity on LDH, whereas some of them displayed a certain inhibition activity on MAGL. In particular, compound **1** was the most active on MAGL, showing an IC_{50} value of 88.0 µM, and modeling studies rationalized the supposed binding mode of **1** in the MAGL active site.

Introduction

Cistanche is a genus of Orobanchaceae family including about 20 species, usually holoparasitic desert plants, that lack chlorophyll and obtain their nutrients and water from the roots of host plants that they parasitize. This genus is distributed to certain arid and semiarid regions of Africa, Asia, and the Mediterranean area, including parts of southern Europe [1]. Some *Cistanche* species are used for food application and in the traditional Chinese medicine as tonic for the treatment of kidney deficiency, impotence, infertility, profuse metrorrhagia, and chronic constipation [2]. The secondary metabolites produced by the representatives of the *Cistanche* genus include phenylethanoid glycosides, lignans, iridoids, and oligosaccharides [3–5] some of which have been shown to possess interesting biological activity such as anti-inflammatory, neuroprotective, immunomodulatory, antioxidative, antibacterial, and antiviral properties [2]. *Cistanche phelypaea* (L.) Coutinho syn. *Cistanche tinctoria* (Desf.) Beck is an erect perennial parasite plant, with numerous yellow flowers and absent roots: the plant attaches itself to its host (*Tamarix gallica* L. [Tamaricaceae], *Calligonum comosum* L'Hér [Polygonaceae], and *Pulicaria* sp. [Asteraceae]) through small tubers. In North Africa traditional medicine, it is used for diarrhea, diabetes, intestinal troubles, infection, and as a diuretic [6]. Previous chemical studies revealed the presence of iridoids and phenylethanoids as main constituents [7, 8].

As a part of our research program for characterization of the biological activity of different classes of natural products [9, 10], herein we report the isolation and the structure characterization of four new phenylethanoid glycosides (**1**–**4**) (▶ **Fig. 1**), along with three known compounds from *C. phelypaea* aerial parts. The isolates were assayed for their lactate dehydrogenase (LDH) and monoacylglycerol lipase (MAGL) inhibitory activity. In fact, tumor cells exhibit progressive metabolic changes that are correlated with malignancy. In particular, glycolytic and lipidic pathways are reprogrammed in order to support the rapid growth of proliferating cells [11]. These dysregulated metabolic pathways are typical features of cancer, and at the same time, they may offer therapeutic windows for anticancer agents that target them. In this context, LDH and MAGL are two enzymes overexpressed in tumor tissues, which play key roles in the typical glycolytic and lipidic cancer metabolism, respectively [12, 13]. In particular, the human isoform 5 of the enzyme LDH (*h*LDH5), made of four A subunits, catalyzes the final step of glycolysis, which consists in the reduction of pyruvate to lactate, thus allowing the adenosine triphosphate production in cancer cells that rely on glycolysis for their survival. Glycolytic cancer cells display high glucose uptake and elevated lactate production, and the overexpression of specific enzymes such as LDH is necessary to assure a sufficient energy production. Therefore, the inhibition of this crucial enzyme may be considered a promising strategy to counteract cancer invasiveness, without affecting normal cells, which instead use oxidative phosphorylation for most of their purposes. On the other hand, MAGL is a serine hydrolase that cleaves monoacyglycerols into fatty acids and glycerol. In particular, MAGL is the lipolytic enzyme that is mainly responsible for the degradation of the endocannabinoid 2-arachidonoylglycerol, which is a neurotransmitter and an important intermediate in lipid metabolism involved in many physiological processes. Moreover, the intensified production of fatty acids in cancer cells, generated by MAGL activity, increases the formation of protumorigenic signaling molecules [14]. Therefore, MAGL represents a potential target to treat diverse pathological conditions, including cancer. In the last decades, a great effort has been directed toward the identification of small molecules that are able to inhibit LDH [15, 16] or MAGL [17, 18], and many compounds displaying efficient inhibitory activity on these targets were either discovered from natural sources or obtained by chemical synthesis. Therefore, the search for LDH or MAGL inhibitors represents an attractive goal to find new effective anticancer drugs interfering with the peculiar cancer metabolism and, therefore, has prompted us to carry out the investigation herein reported.

Results and Discussion

The phytochemical study of *C. phelypaea n*-butanol extract, after submission to flash column chromatography followed by RP-HPLC, afforded four new phenylethanoid glycosides (**1**–**4**) (▶ **Fig. 1**) and three known compounds, named brandioside [19], pinoresinol 4-*O*-*β*-D-glucopyranoside [20], and apigenin 7-*O*-*β*-glucuronopyranoside [21] by comparison of NMR and MS data with those reported in the literature.

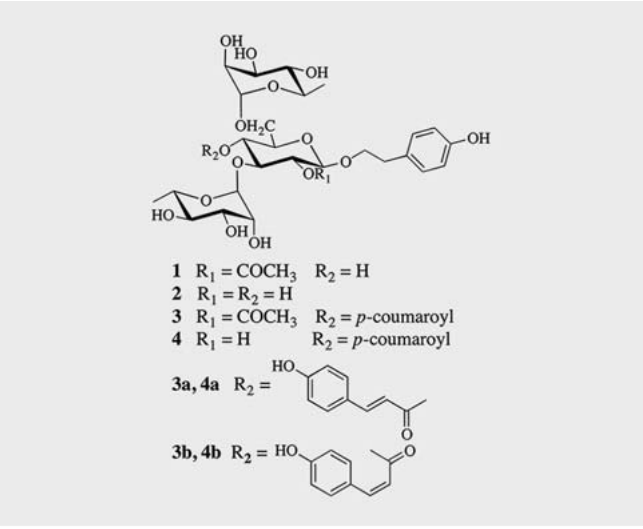

▶ **Fig. 1** Chemical structures of compounds **1**–**4** isolated from *C. phelypaea* aerial parts.

Compound **1** was obtained as a brownish amorphous solid with a molecular formula $C_{28}H_{42}O_{16}$, as determined by ^{13}C NMR and HRESIMS analyses (*m/z* 657.2353 $[M + Na]^+$). The positive ESIMS spectrum showed a sodiated molecular ion peak at *m/z* 657 $[M + Na]^+$, while its fragmentation pattern was characterized by peaks at *m/z* 597 $[M + Na - 60]^+$, 511 $[M + Na - 146]^+$, and 365 $[M + Na - 146 - 146]^+$, due to the subsequent loss of an acetyl group and two deoxyhexose units, respectively. The ^1H NMR spectra of **1** (▶ **Table 1**) exhibited characteristic signals of *ortho*-coupled A_2B_2 type aromatic protons at *δ* 6.71 (2H, d, *J* = 8.0 Hz) and 7.04 (2H, d, *J* = 8.0 Hz), three anomeric protons at *δ* 4.44 (1H, d, *J* = 8.0 Hz), 4.76 (1H, d, *J* = 1.3 Hz), and 4.80 (1H, d, *J* = 1.5 Hz), an acetyl group at *δ* 2.00 (3H, s), two methyl groups at *δ* 1.26 (3H, d, *J* = 6.3 Hz) and 1.27 (3H, d, *J* = 6.5 Hz), and two methylenes at *δ* 4.04 (1H, m), 3.62 (1H, m), and 2.80 (2H, m). This evidence suggested the presence of a phenylethanol residue and three sugar moieties [5]. The observation of ^{13}C NMR spectrum (▶ **Table 1**) confirmed these findings. The structures of the sugar units were assigned by 1D TOCSY and 2D NMR experiments, indicating the presence of one *β*-glucopyranoside and two *α*-rhamnopyranosyl residues. The complete assignments of all protons and carbons were based by the analysis of HSQC, COSY, and HMBC data, indicating that the two rhamnopyranosyl units were terminal units. The relative configuration of the anomeric carbon of the glucose residue was deduced to be *β* from the coupling constant (*J* = 8.0 Hz) of the anomeric proton. In the case of the rhamnose residue, the *α* anomeric configuration was derived by comparison of the pertinent ^{13}C NMR data with those reported in literature [9]. The configuration of the sugar units was assigned after hydrolysis of **1** with 1 N HCl. The hydrolyzate was trimethylsilylated, and GC retention times of each sugar were compared with those of authentic samples prepared in the same manner. The HMBC spectrum of **1** displayed the correlations between the proton signal at δ_H 4.44 (H-1_{glc}) and carbon resonance at δ_C 72.5 (C-8), confirming that the phenylethanol moiety was linked to C-1_{glc}. Simi-

▶ **Table 1** ^{1}H and ^{13}C-NMR data of compounds **1–4** (CD_3OD, 600 MHz, *J* in Hz).

Position	1		2		3a/3b		4a/4b	
	δ_H	δ_C	δ_H	δ_C	δ_H	δ_C	δ_H	δ_C
1		131.0		131.0		131.7		130.7
2/6	7.04 d (8.0)	131.2	7.07 d (8.0)	131.5	7.05 d (8.0)	131.3	7.10 d (8.0)	130.9
3/5	6.71 d (8.0)	116.3	6.72 d (8.0)	116.4	6.73 d (8.0)	116.2	6.73 d (8.0)	116.2
4		157.0		157.1		157.0		157.1
7	2.80 m	36.4	2.85 m	37.6	2.78 m	36.0	2.86 m	36.7
8a	4.04 m	72.5	3.99 m	72.0	4.06 m	72.3	4.02 m	72.7
8b	3.62 m		3.74 m		3.65 m		3.75 m	
glc-1	4.44 d (8.0)	103.2	4.34 d (7.8)	104.6	4.55 d (7.8)	102.1	4.40 d (8.0)	104.6
2	4.78 dd (9.0, 8.0)	75.0	3.29 dd (9.5, 7.8)	75.0	4.88 dd (9.5, 7.8)	74.3	3.40 dd (9.5, 8.0)	76.4
3	3.65 t (9.0)	83.1	3.50 t (9.5)	83.8	4.03 t (9.5)	80.8	3.83 t (9.5)	81.9
4	3.44 t (9.0)	70.1	3.35[a]	70.0	5.12 t (9.5)	69.3	5.00 t (9.5)	70.2
5	3.46 m	77.1	3.43 m	76.3	3.77 m	75.2	3.70 m	74.9
6a	4.00 dd (12.0, 3.0)	68.0	3.99 dd (12.0, 3.0)	68.0	3.79 dd (12.0, 3.0)	67.5	3.77 dd (12.0, 3.5)	67.8
6b	3.68 dd (12.0, 4.5)		3.65 dd (12.0, 5.0)		3.50 dd (12.0, 5.0)		3.49 dd (12.0, 4.5)	
$\underline{CO}CH_3$		171.3				171.6		
$CO\underline{CH_3}$	2.00 s	21.2			1.98 s	21.4		
$rha_I - 1$	4.76 d (1.3)	102.1	5.21 d (2.0)	100.8	4.77 d (1.8)	103.3	5.21 d (2.0)	102.7
2	3.83 dd (3.0, 1.8)	72.8	3.96 dd (3.0, 2.0)	71.6	3.74 dd (3.0, 1.8)	71.7	3.94 dd (3.0, 2.0)	72.4
3	3.96 dd (9.0, 3.0)	72.0	3.70 dd (9.0, 3.0)	70.7	3.54 dd (9.0, 3.0)	72.0	3.60 dd (9.0, 3.0)	72.7
4	3.39 t (9.0)	74.3	3.39 t (9.0)	73.4	3.29 t (9.0)	73.0	3.31 t (9.0)	74.2
5	3.68 m	70.7	3.69 m	71.2	3.54 m	70.2	3.58 m	70.6
6	1.26 d (6.3)	18.1	1.26 d (6.5)	18.3	1.08 d (6.5)	18.7	1.09 d (6.0)	18.3
$rha_{II} - 1$	4.80 d (1.5)	102.5	4.76 d (1.8)	101.6	4.63 d (2.0)	102.5	4.65 d (2.0)	101.1
2	3.83 dd (3.0, 1.8)	72.6	3.85 dd (3.5, 1.8)	71.5	3.89 dd (3.5, 2.0)	71.4	3.86 dd (3.5, 2.0)	72.3
3	3.96 dd (9.0, 3.0)	72.4	3.70 dd (9.0, 3.5)	72.3	3.70 dd (9.0, 3.5)	72.0	3.75 dd (9.0, 3.5)	72.6
4	3.39 t (9.0)	74.0	3.40 t (9.0)	74.0	3.37 t (9.0)	73.2	3.34[a]	74.0
5	3.68 m	70.6	3.99 m	70.0	3.64 m	69.3	3.66 m	70.7
6	1.27 d (6.5)	18.3	1.27 d (6.5)	18.1	1.22 d (6.0)	18.3	1.21 d (6.0)	18.5
p-coum-1						127.3		127.4
2/6 *trans*					7.44 d (8.0)	131.3	7.50 d (7.8)	130.9
2/6 *cis*					7.75 d (8.0)	134.6	7.72 d (7.8)	133.4
3/5 *trans*					6.84 d (8.0)	116.2	6.83 d (7.8)	116.2
3/5 *cis*					6.80 d (8.0)	115.3	6.80 d (7.8)	115.2
4						162.0		161.7
α-trans					6.37 d (16.0)	114.9	6.38 d (16.0)	114.0
α-cis					5.83 d (12.0)	115.9	5.83 d (12.0)	115.2
β-trans					7.70 d (16.0)	148.1	7.71 d (16.0)	147.3
β-cis					6.97 d (12.0)	147.7	6.99 d (12.0)	146.4
COO						168.0		168.0

J values are in parentheses and reported in Hz. Chemical shifts are given in ppm. Assignments were confirmed by COSY, 1D-TOCSY, HSQC, and HMBC experiments. Glc: *β*-D-glucopyranoside; rha: *α*-L-rhamnopyranosyl; *p*-coum: *p*-coumaroyl; [a] overlapped signal.

larly, the correlation between signals at δ_H 4.78 (H-2_{glc}) and δ_C 171.3 suggested that the acetyl group was linked to C-2_{glc}. Likewise, the long-range correlations between δ_H 4.76 (H-1_{rhaI}) and carbon resonance δ_C 83.1 (C-3_{glc}), δ_H 4.80 (H-1_{rhaII}), and δ_C 68.0 (C-6_{glc}) allowed to establish that the two *α*-L-rhamnopyranosyl moieties were linked at C-3_{glc} and C-6_{glc}, respectively. Thus, the

structure of **1** was established as 1-*β*-*p*-hydroxyphenyl-ethyl-2-*O*-acetyl-3,6-di-*α*-L-rhamnopyranosyl-*β*-D-glucopyranoside.

The molecular formula of compound **2**, isolated as a brownish amorphous solid, was assigned $C_{26}H_{40}O_{15}$, as deduced by HRESIMS analyses (*m/z* 615.2232 $[M + Na]^+$), as well as from ^{13}C NMR data. The ESIMS/MS spectrum displayed two fragments at *m/z* 469 $[M + Na - 146]^+$ and 323 $[M + Na - 146 - 146]^+$ attributable to the subsequent loss of two deoxyhexose units, respectively. Comparison of ^1H and ^{13}C NMR spectra of **2** (▶ **Table 1**) with those of **1** revealed **2** to differ from **1** only for the absence of the acetyl group at C-2 of glucose unit. Thus, the structure of **2** was determined as 1-*β*-*p*-hydroxyphenyl-ethyl-3,6-*O*-di-*α*-L-rhamnopyranosyl-*β*-D-glucopyranoside.

Compound **3** displayed a molecular formula $C_{37}H_{48}O_{18}$ by HRESIMS (*m/z* 803.2715 $[M + Na]^+$). The ESIMS of **3** showed a sodiated molecular ion peak at *m/z* 803 $[M + Na]^+$ and a fragmentation pattern with peaks at *m/z* 743 $[M + Na - 60]^+$, 657 $[M + Na - 146]^+$, and 511 $[M + Na - 146 - 146]^+$, corresponding to the subsequent loss of an acetyl moiety and two deoxyhexose units. Analysis of NMR data of **3** (▶ **Table 1**), besides chemical shifts similar to those of **1**, displayed the presence of two couples of signals attributable to *trans*-olefinic protons at *δ* 6.37 (1H, d, *J* = 16.0 Hz, H-α_{trans}) and 7.70 (1H, d, *J* = 16.0 Hz, H-β_{trans}), *cis*-olefinic protons at *δ* 5.83 (1H, d, *J* = 12.0 Hz, H-α_{cis}), and 6.97 (1H, d, *J* = 12.0 Hz, H-β_{cis}), and two couples of *ortho*-coupled A_2B_2 aromatic protons at *δ* 6.84 (2H, d, *J* = 8.0 Hz, H-3/H-5$_{trans}$) and 7.44 (2H, d, *J* = 8.0 Hz, H-2/H-6$_{trans}$), and 6.80 (2H, d, *J* = 8.0 Hz, H-3/H-5$_{cis}$) and 7.75 (2H, d, *J* = 8.0 Hz, H-2/H-6$_{cis}$). Also in this case the assignments of all proton and carbon signals were deduced from a combined analysis of 1D and 2D NMR experiments. Moreover, key correlation peaks in the HMBC spectrum of **3** between the proton signal at δ_H 5.12 (H-4$_{glc}$) and carbon resonance at δ_C 168.0 (COO), δ_H 4.88 (H-2$_{glc}$), and δ_C 171.6 ($\underline{CO}CH_3$) were present, confirming that the *p*-coumaroyl group was linked to C-4$_{glc}$ while the acetyl group at C-2$_{glc}$. Thus, compound **3** was identified as an inseparable mixture 7:3 of 1-*β*-*p*-hydroxyphenyl-ethyl-2-*O*-acetyl-3,6-di-*α*-L-rhamnopyranosyl-4-*trans*-*p*-coumaroyl-*β*-D-glucopyranoside (**3a**) and 1-*β*-*p*-hydroxyphenyl-ethyl-2-*O*-acetyl-3,6-di-*α*-L-rhamnopyranosyl-4-*cis*-*p*-coumaroyl-*β*-D-glucopyranoside (**3b**).

The HRESIMS of compound **4**, a brownish amorphous solid, showed a sodiated molecular ion peak at *m/z* 761.2604 $[M + Na]^+$, corresponding to the molecular formula $C_{35}H_{46}O_{17}$. In the ESIMS/MS fragmentation pattern of *m/z* 761 $[M + Na]^+$, peaks at *m/z* 615 $[M + Na - 146]^+$ and 469 $[M + Na - 146 - 146]^+$, due to the subsequent loss of two deoxyhexose units, respectively, were evident. Comparison of NMR data of **4** (▶ **Table 1**) with those of **3** showed in **4** the absence of the acetyl group at C-2$_{glc}$. In the light of these data, compound **4** was established to be an inseparable mixture 7:3 of 1-*β*-*p*-hydroxyphenyl-ethyl-3,6-di-*α*-L-rhamnopyranosyl-4-*trans*-*p*-coumaroyl-*β*-D-glucopyranoside (**4a**) and 1-*β*-*p*-hydroxyphenyl-ethyl-3,6-di-*α*-L-rhamnopyranosyl-4-*cis*-*p*-coumaroyl-*β*-D-glucopyranoside (**4b**).

Phenylethanoids **1**–**4**, pinoresinol 4-*O*-*β*-D-glucopyranoside, brandioside, and apigenin 7-*O*-*β*-glucuronopyranoside, were assayed on human LDH5 and MAGL purified isoforms to determine their inhibition potencies (▶ **Table 2**). All the compounds were inactive on *h*LDH5, showing IC_{50} values greater than 200 µM, thus being less potent than reference compound galloflavin [22]. In *h*MAGL enzymatic assays, only two derivatives (compound **4** and apigenin 7-*O*-*β*-glucuronopyranoside) proved to be inactive, whereas pinoresinol 4-*O*-*β*-D-glucopyranoside and brandioside exhibited IC_{50} values of 130.2 and 156.1 µM, respectively. Compounds **2** and **3** showed a better inhibition activity, with similar IC_{50} values of 117.4 and 113.9 µM, respectively. The best inhibition potency on *h*MAGL was demonstrated by compound **1**, with an IC_{50} value in the low micromolar range (88.0 µM), and it proved to be selective for *h*MAGL over *h*LDH. Although its inhibition activity was lower than reference MAGL synthetic inhibitor (4-[4-chlorobenzoyl]piperidin-1-yl)(4-methoxyphenyl)-methanone (compound "CL6a" [17]), this natural compound is the first phenylethanoid, bearing *β*-D-glucopyranosyl and *α*-L-rhamnopyranosyl sugar units, displaying a promising activity on *h*MAGL. Presently, only few compounds derived from natural sources have shown an inhibitory activity on this enzyme [23]; however, they belong to different chemical classes.

▶ **Table 2** *h*LDH5 and *h*MAGL inhibition potencies.

Compound	IC_{50} (µM)			
	***h*LDH5**	**CI (95%, n = 3)**	***h*MAGL**	**CI (95%, n = 3)**
1	> 200	–	88.0	[60.7, 127.6]
2	> 200	–	117.4	[95.0, 145.1]
3a/3b	> 200	–	113.9	[93.8, 138.4]
4a/4b	> 200	–	> 200	–
pinoresinol 4-*O*-*β*-D-glucopyranoside	> 200	–	130.2	[110.2, 153.8]
brandioside	> 200	–	156.1	[151.1, 164.7]
apigenin 7-*O*-*β*-glucuronopyranoside	> 200	–	> 200	–
galloflavin	110.1	[82.9, 146.2]	–[a]	–
CL6a	–[a]	–	12.1	[8.9, 16.3]

CI: confidence interval; [a] not tested.

In order to better characterize the binding mode of compound **1** into MAGL, its complex with the target protein was subjected to docking calculations. In particular, the putative binding pose emerging from these modeling studies showed that the sugar moiety lies in the wide lipophilic cavity of the protein forming lipophilic interactions with L148, L213, L241, and V183, whereas the *p*-hydroxyphenyl-ethyl ring lies into the small pocket of the binding site and forms lipophilic interactions with residues Y194 and V270 (▶ **Fig. 2**). A high number of H-bonds stabilizes the binding disposition of compound **1**: the carbonyl group of the *O*-acetyl group linked to the glucopyranoside forms two H-bonds with the backbone nitrogen of A51 and M123 and the 4-OH of

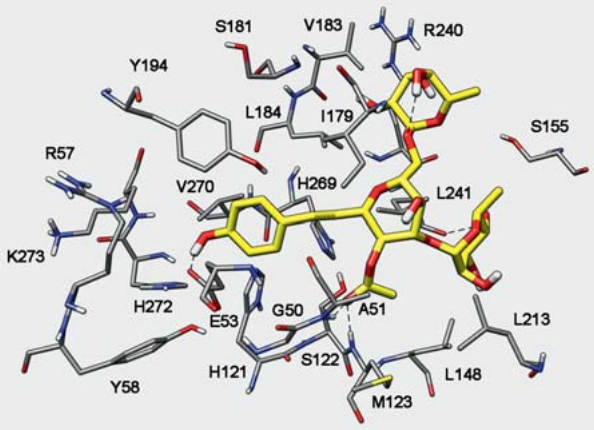

▶ **Fig. 2** View of the most relevant ligand-receptor interactions of the **1**-*h*MAGL complex. Hydrogen bonds are represented as black dashed lines.

the 3-*α*-L-rhamnopyranoside forms an H-bond with the oxygen backbone of L241. Compound **1** is also characterized by an intramolecular H-bond between the ethereal oxygen of the 6-*α*-L-rhamnopyranoside and the 4-OH of the same portion. Furthermore, the OH group of the *p*-hydroxyphenyl-ethyl portion forms an H-bond with residue E53, in which it behaves as a H-bond donor.

In summary, seven compounds, including four new structures (**1**–**4**), were isolated and characterized from the aerial parts of *C. phelypaea*. The isolation and structural characterization of the new phenylethanoids **1**–**4** and the known compound pinoresinol 4-*O*-*β*-D-glucopyranoside are completely in agreement with the available information on the chemical types of secondary metabolites typical of *Cistanche* species [24, 25], while brandioside and apigenin 7-*O*-*β*-glucuronopyranoside are reported from this genus for the first time here. Moreover, to our knowledge this is the first report of naturally occurring phenyletanoid as a MAGL inhibitor. This study will open the way for future investigation on plant glycosylated small molecules as potential MAGL inhibitors. HRESIMS and NMR spectra of compounds **1**–**4** and data for the IC_{50} determination of compound **1** in MAGL enzymatic assays are available as Supporting Information.

Materials and Methods

General experimental procedures

Optical rotations were measured on an Atago AP-300 digital polarimeter equipped with a sodium lamp (589 nm) and a 1-dm microcell. NMR experiments were recorded at 300 K in CD_3OD on a Bruker DRX-600 spectrometer (Bruker BioSpin GmBH) equipped with a Bruker 5 mm TCI CryoProbe as reported previously [26]. HRESIMS were acquired in the positive ion mode on a LTQ Orbitrap XL mass spectrometer (Thermo Fisher Scientific). ESIMS were obtained from an LCQ Advantage ThermoFinnigan spectrometer (ThermoFinnigan), equipped with a Xcalibur software. Column chromatography was performed over Sephadex LH-20 (40–70 µm, Pharmacia) at a flow rate 0.8 mL/min. HPLC separations were conducted on a Shimadzu LC-8A series pumping system equipped with a Shimadzu RID-10A refractive index detector and Shimadzu injector on a C_{18} µ-Bondapak column (30 cm × 7.8 mm, 10 µm Waters, flow rate 2.0 mL/min). TLC analyses were carried out using glass-coated silica gel 60 F_{254} (0.20 mm thickness) plates (Merck) with $CHCl_3$-MeOH-H_2O (70 : 30 : 3) as eluent and cerium sulphate as spray reagent. GC analysis was performed using a Dani GC 1000 instrument on a L-CP-Chirasil-Val column (0.32 mm × 25 m) working with the following temperature program: 100 °C for 1 min, ramp of 5 °C/min up to 180 °C; injector and detector temperature 200 °C; carrier gas N_2 (2.0 mL/min); detector dual FID; split ratio 1 : 30; injection 5 µL.

Plant material

C. phelypaea aerial parts were collected in March 2012 in the southwest of Algeria. The plant was identified by Prof. Gérard De Bélair, Faculty of Sciences, University of Annaba, Algeria. A voucher specimen (number Ct.03.12) has been deposited in the Herbarium of the Department of Chemistry, Université des Frères Mentouri-Constantine, Constantine, Algeria.

Extraction and isolation

The dried and powdered aerial parts (4 kg) of *C. phelypeae* were extracted with MeOH-H_2O (4 : 1) at room temperature for 48 h. The extraction was repeated three times by changing the solvent. The obtained extract was filtered, concentrated, and successively extracted with petroleum ether, chloroform, ethyl acetate and *n*-butanol, to give 3.27, 4.87, 10.96, and 36.86 g of the respective residues. The *n*-butanol extract (10.59 g) was subjected to column chromatography over Sephadex LH-20 in MeOH. Fractions of 12 mL were collected, analyzed by TLC, and grouped to give 11 major fractions (A–K). Fraction K contained pure apigenin 7-*O*-*β*-D-glucuronopyranoside (28 mg). Fraction B (245.1 mg) was purified by RP-HPLC with MeOH-H_2O (3 : 7) as eluent to obtain pure compound **1** (7.9 mg, t_R 21 min). Fraction C (896.8 mg) was purified by RP-HPLC with MeOH-H_2O (25 : 75) as eluent to afford pure compound **2** (6.3 mg, t_R 15 min). Fraction E (638.9 mg) was purified by RP-HPLC with MeOH-H_2O (45 : 55) as eluent to give brandioside (7 mg, t_R 15 min) and compounds **4** (14.9 mg, t_R 20 min) and **3** (11.1 mg, t_R 34 min). Fraction G (172.6 mg) was purified by RP-HPLC with MeOH-H_2O (35 : 65) as eluent to obtain pinoresinol 4-*O*-*β*-D-glucopyranoside (3.6 mg, t_R 18 min).

Compound ***1***: brownish amorphous solid; $[\alpha]_D^{25}$ −58.5 (c 0.1, MeOH); UV (MeOH) λ_{max} (log ε): 223 (4.20), 280 (3.50), 321 (3.06); ^1H and ^{13}C NMR data, see ▶ **Table 1**; ESIMS *m/z* 657 $[M + Na]^+$, 597 $[M + Na - 60]^+$, 511 $[M + Na - 146]^+$, 451 $[M + Na - 60 - 146]^+$, 365 $[M + Na - 146 - 146]^+$; HRESIMS: *m/z* 657.2353 $[M + Na]^+$ (calcd. for $C_{28}H_{42}NaO_{16}$, *m/z* 657.2371).

Compound ***2***: brownish amorphous solid; $[\alpha]_D^{25}$ −7.0 (c 0.1, MeOH); UV (MeOH) λ_{max} (log ε): 222 (4.09), 280 (3.55), 315 (3.10); ^1H and ^{13}C NMR data, see ▶ **Table 1**; ESIMS *m/z* 615 $[M + Na]^+$, 469 $[M + Na - 146]^+$, 323 $[M + Na - 146 - 146]^+$; HRESIMS: *m/z* 615.2232 $[M + Na]^+$ (calcd. for $C_{26}H_{40}NaO_{15}$, *m/z* 615.2265).

Compound ***3***: brownish amorphous solid; $[\alpha]_D^{25}$ −96 (c 0.1, MeOH); UV (MeOH) λ_{max} (log ε): 225 (4.26), 316 (3.87); ^1H and

^{13}C NMR data, see ▶ **Table 1**; ESIMS *m/z* 803 $[M + Na]^+$, 743 $[M + Na - 60]^+$, 657 $[M + Na - 146]^+$, 511 $[M + Na - 146 - 146]^+$; HRESIMS: *m/z* 803.2715 $[M + Na]^+$ (calcd. for $C_{37}H_{48}NaO_{18}$, *m/z* 803.2738).

Compound ***4***: brownish amorphous solid; $[\alpha]_D^{25}$ −85.5 (c 0.1, MeOH); UV (MeOH) λ_{max} (log ε): 224 (4.30), 315 (3.85); ^{1}H and ^{13}C NMR data, see ▶ **Table 1**; ESIMS *m/z* 761 $[M + Na]^+$, 615 $[M + Na - 146]^+$, 469 $[M + Na - 146 - 146]^+$; HRESIMS: *m/z* 761.2604 $[M + Na]^+$ (calcd. for $C_{35}H_{46}NaO_{17}$, *m/z* 761.2633).

Acid hydrolysis of compounds 1–4

A solution of each compound (2.0 mg) in 1 N HCl (1 mL) was stirred at 80 °C in a stoppered reaction vial for 4 h. After cooling, the solution was evaporated under a stream of N_2. The residue was dissolved in 1-(trimethylsilyl)imidazole and pyridine (0.2 mL, 1 : 1), and the solution was stirred at 60 °C for 5 min. After drying the solution, the residue was partitioned between H_2O and $CHCl_3$. The $CHCl_3$ layer was analyzed by GC using a L-CP-Chirasil-Val column (0.32 mm × 25 m). Temperatures of both the injector and detector was 200 °C. A temperature gradient system was used for the oven, starting at 100 °C for 1 min and increasing up to 180 °C at a rate of 5 °C/min. Peaks of the hydrolysate were detected by comparison with retention times of authentic samples of D-glucose and L-rhamnose (Sigma-Aldrich) after treatment with 1-(trimethylsilyl)imidazole in pyridine.

Enzymatic assays

All the compounds were assayed against purified *h*LDH5 (Lee Biosolution Inc.) and *h*MAGL (Cayman Chemical), as previously reported [15, 17]. The reference MAGL synthetic inhibitor (4-[4-chlorobenzoyl]piperidin-1-yl)(4-methoxyphenyl)-methanone (compound "CL6a") was synthesized in our laboratory (purity percentage 99 % by HPLC analysis), as previously reported [17]. Both assays were performed in 96-well plates at room temperature at a final volume of 200 µL. Compounds were dissolved in DMSO stock solutions at the maximum concentration of 625 µM (the concentration of DMSO did not exceed 4 % during the measurements), and this solution was diluted to seven different concentrations (from 625 to 0.86 µM, in duplicate for each concentration) that were used to generate the concentration-response curve. All the IC_{50} values are the mean of three independent experiments. Maximum and minimum controls were also included in each plate. The enzymatic reaction for LDH assays was performed in the "forward" direction (pyruvate to lactate), and the amount of consumed NADH was monitored (340 nm). Assays were performed in 100 mM phosphate buffer (pH = 7.4) in the presence of 200 µM pyruvate and 40 µM NADH. After 15 min of incubation, the final measurements were carried out by using a Victor X3 microplate reader (PerkinElmer). IC_{50} values were derived from experimental data using the sigmoidal dose-response fitting of GraphPad Prism software. The enzymatic reaction for MAGL assays was based on the conversion of the substrate 4-nitrophenylacetate (4-NPA) to 4-nitrophenol and the amount of produced 4-nitrophenol was monitored (405 nm), as previously reported [27]. Assays were performed in 10 mM Tris buffer (pH = 7.2), containing 1 mM EDTA and 0.1 mg/mL BSA, in the presence of 100 µM 4-NPA. After the reaction had proceeded for 30 min, absorbance values were then measured by using a Victor X3 microplate reader (PerkinElmer). IC_{50} values were derived from experimental data using the sigmoidal dose-response fitting of GraphPad Prism software.

Docking studies

The crystal structure of *h*MAGL (pdb code 3PE6 [28]) was sourced from the Protein Data Bank [29]. First we added hydrogen atoms. Then the protein complexed with its reference inhibitor was minimized using Amber14 software [30] and ff14SB force field at 300 K. The complex was placed in a rectangular parallelepiped water box, an explicit solvent model for water (TIP3P) was used, and the complex was solvated with a 10 Å water cap. To neutralize the system, sodium ions as counterions were added. Then two steps of minimization were carried out. First, the protein was kept fixed with a position restraint of 500 kcal/mol·Å2 and only the positions of the water molecules were minimized. Second, the entire system through 5000 steps of steepest descent followed by a CG was minimized until a convergence of 0.05 kcal/Å·mol was reached. The ligands were built using Maestro [31] and minimized by means of Macromodel [32] in a water environment, following the CG method to obtain a convergence value of 0.05 kcal/Å·mol, using the MMFF's force field and a distance-dependent dielectric constant of 1.0. Automated docking was carried out by means of the AutoDock 4.0 program [33]; AutoDock Tools [34] was used to identify the torsion angles in the ligands, add the solvent model, and assign the Kollman atomic charges to the protein. The ligand charge was calculated using the Gasteiger method. By considering the ZYH [(2-cyclohexylbenzo[d]oxazol-6-yl)(3-(4-(pyrimidin-2-yl)piperazin-1-yl)azetidin-1-yl)methanone] reference inhibitor as the central group, the regions of interest used were defined by AutoDock; in particular a grid of 82, 40, and 30 points in the x, y, and z directions, centered on the core of the mass of this compound, was constructed. For the energetic map calculations, a grid spacing of 0.375 Å and a distance-dependent function of the dielectric constant were used. With the aid of the Lamarckian Genetic Algorithm, the docked compounds were subjected to 100 runs of the AutoDock search, using 500 000 steps of energy evaluation and the default values of the other parameters. The cluster analysis on the results was performed using an RMS tolerance of 2.0 Å.

Supporting Information

HRESIMS and NMR spectra of compounds **1**–**4** and data for the IC_{50} determination of compound **1** in MAGL enzymatic assays are available as Supporting Information.

Acknowledgements

The authors are grateful to Algerian Ministry of Higher Education and Research (MESR) for the PNE grant to Miss Khadidja Aya Beladjila.

Conflict of Interest

The authors declare no conflicts of interest.

References

[1] Fahmy GM, El-Tantawi H, Abd El-Ghani MM. Distribution, host range and biomass of two species of *Cistanche* and *Orobanche cernua* parasitizing the roots of some Egyptian xerophytes. J Arid Environ 1996; 34: 263–276

[2] Wang LI, Ding H, Yu HS, Han LF, Lai QH, Zhang LJ, Song XB. *Cistanche herba*: chemical constituents and pharmacological effects. Chin Herb Med 2015; 7: 135–142

[3] Xiong Q, Kadota S, Tani T, Namba T. Antioxidative effects of phenylethanoids from *Cistanche deserticola*. Biol Pharm Bull 1996; 19: 1580–1585

[4] Morikawa T, Pan Y, Ninomiya K, Imura K, Yuan D, Yoshikawa M, Hayakawa T, Muraoka O. Iridoid and acyclic monoterpene glycosides, kankanosides L, M, N, O, and P from *Cistanche tubulosa*. Chem Pharma Bull 2010; 58: 1403–1410

[5] Liu XM, Li J, Jiang Y, Zhao MB, Tu PF. Chemical constituents from *Cistanche sinesis* (Orobanchaceae). Biochem Syst Ecol 2013; 47: 21–24

[6] Boulous L. Medicinal Plants of North Africa. Michigan: Reference Publication Algonc; 1983: 286

[7] Melek FR, El-Shabrawy OA, El-Gindy M, Miyase T, Hilal SH. Pharmacological activity and composition of the ethyl acetate extract of *Cistanche phelypaea*. Fitoterapia 1993; 64: 11–14

[8] Deyama T, Yahikozawa K, Al-Easa HS, Rizk AM. Constituents of plants growing in Qatar: part XXXVIII. Constituents of *Cistanche phelypaea*. Qatar University Sci J 1995; 15: 51–55

[9] Bader A, Tuccinardi T, Granchi C, Martinelli A, Macchia M, Minutolo F, De Tommasi N, Braca A. Phenylpropanoids and flavonoids from *Phlomis kurdica* as inhibitors of human lactate dehydrogenase. Phytochemistry 2015; 116: 262–268

[10] De Leo M, Peruzzi L, Granchi C, Tuccinardi T, Minutolo F, De Tommasi N, Braca A. Constituents of *Polygala flavescens* ssp. *flavescens* and their activity as inhibitors of human lactate dehydrogenase. J Nat Prod 2017; 80: 2077–2087

[11] Deberardinis RJ, Sayed N, Ditsworth D, Thompson CB. Brick by brick: metabolism and tumor cell growth. Curr Opin Genet Dev 2008; 18: 54–61

[12] Nomura DK, Long JZ, Niessen S, Hoover HS, Ng SW, Cravatt BF. Monoacylglycerol lipase regulates a fatty acid network that promotes cancer pathogenesis. Cell 2010; 140: 49–61

[13] Fiume L, Manerba M, Vettraino M, Di Stefano G. Inhibition of lactate dehydrogenase activity as an approach to cancer therapy. Future Med Chem 2014; 6: 429–445

[14] Nomura DK, Lombardi DP, Chang JW, Niessen S, Ward AM, Long JZ, Hoover HH, Cravatt BF. Monoacylglycerol lipase exerts dual control over endocannabinoid and fatty acid pathways to support prostate cancer. Chem Biol 2011; 18: 846–856

[15] Granchi C, Roy S, Del Fiandra C, Tuccinardi T, Lanza M, Betti L, Giannaccini G, Lucacchini A, Martinelli A, Macchia M, Minutolo F. Triazole-substituted *N*-hydroxyindol-2-carboxylates as inhibitors of isoform 5 of human lactate dehydrogenase (*h*LDH5). Medchemcomm 2011; 2: 638–643

[16] Purkey HE, Robarge K, Chen J, Chen Z, Corson LB, Ding CZ, DiPasquale AG, Dragovich PS, Eigenbrot C, Evangelista M, Fauber BP, Gao Z, Ge H, Hitz A, Ho Q, Labadie SS, Lai KW, Liu W, Liu Y, Li C, Ma S, Malek S, O'Brien T, Pang J, Peterson D, Salphati L, Sideris S, Ultsch M, Wei B, Yen I, Yue Q, Zhang H, Zhou A. Cell active hydroxylactam inhibitors of human lactate dehydrogenase with oral bioavailability in mice. ACS Med Chem Lett 2016; 7: 896–901

[17] Tuccinardi T, Granchi C, Rizzolio F, Caligiuri I, Battistello V, Toffoli G, Minutolo F, Macchia M, Martinelli A. Identification and characterization of a new reversible MAGL inhibitor. Bioorg Med Chem 2014; 22: 3285–3291

[18] Hernández-Torres G, Cipriano M, Hedén E, Björklund E, Canales Á, Zian D, Feliú A, Mecha M, Guaza C, Fowler CJ, Ortega-Gutiérrez S, López-Rodríguez ML. A reversible and selective inhibitor of monoacylglycerol lipase ameliorates multiple sclerosis. Angew Chem Int Ed Engl 2014; 53: 13765–13770

[19] He ZD, Yang CR. Brandioside, a phenylpropanoid glycoside from *Brandisia hancei*. Phytochemistry 1991; 30: 701–706

[20] Casabuono AC, Pomillo AB. Lignans and a stilbene from *Festuca argentina*. Phytochemistry 1994; 35: 479–483

[21] Flamini G, Antognoli E, Marelli I. Two flavonoids and other compounds from aerial parts of *Centaurea bracteata* from Italy. Phytochemistry 2001; 57: 559–564

[22] Manerba M, Vettraino M, Fiume L, Di Stefano G, Sartini A, Giacomini E, Buonfiglio R, Roberti M, Recanatini M. Galloflavin (CAS 568-80-9): a novel inhibitor of lactate dehydrogenase. ChemMedChem 2012; 7: 311–317

[23] Scalvini L, Piomelli D, Mor M. Monoglyceride lipase: structure and inhibitors. Chem Phys Lipids 2016; 197: 13–24

[24] Kobayashi H, Karasawa H, Miyase T, Fukushima S. Studies on the constituents of *Cistanchis* herba. III. Isolation and structures of new phenylpropanoid glycosides, cistanosides A and B. Chem Pharm Bull 1984; 32: 3009–3014

[25] Yoshizawa F, Deyama T, Takizawa N. The constituents of *Cistanche tubulosa* (SCHRENK) HOOK. f. II.: isolation and structures of a new phenylethanoid glycoside and a new neolignan glycoside. Chem Pharm Bull 1990; 38: 1927–1930

[26] Milella L, Milazzo S, De Leo M, Vera Saltos MB, Faraone I, Tuccinardi T, Lapillo M, De Tommasi N, Braca A. α-Glucosidase and α-amylase inhibitors from *Arcytophyllum thymifolium*. J Nat Prod 2016; 79: 2104–2112

[27] Granchi C, Caligiuri I, Bertelli E, Poli G, Rizzolio F, Macchia M, Martinelli A, Minutolo F, Tuccinardi T. Development of terphenyl-2-methyloxazol-5(4H)-one derivatives as selective reversible MAGL inhibitors. J Enzyme Inhib Med Chem 2017; 32: 1240–1252

[28] Schalk-Hihi C, Schubert C, Alexander R, Bayoumy S, Clemente JC, Deckman I, DesJarlais RL, Dzordzorme KC, Flores CM, Grasberger B, Kranz JK, Lewandowski F, Liu L, Ma H, Maguire D, Macielag MJ, McDonnell ME, Mezzasalma Haarlander T, Miller R, Milligan C, Reynolds C, Kuo LC. Crystal structure of a soluble form of human monoglyceride lipase in complex with an inhibitor at 1.35 Å resolution. Protein Sci 2011; 20: 670–683

[29] Berman HM, Westbrook J, Feng Z, Gilliland G, Bhat TN, Weissig H, Shindyalov IN, Bourne PE. The protein data bank. Nucleic Acids Res 2000; 28: 235–242

[30] Case DA, Berryman JT, Betz RM, Cerutti DS, Cheatham TE III, Darden TA, Duke RE, Giese TJ, Gohlke H, Goetz AW, Homeyer N, Izadi S, Janowski P, Kaus J, Kovalenko A, Lee TS, LeGrand S, Li P, Luchko T, Luo R, Madej B, Merz KM, Monard G, Needham P, Nguyen H, Nguyen HT, Omelyan I, Onufriev A, Roe DR, Roitberg A, Salomon-Ferrer R, Simmerling CL, Smith W, Swails J, Walker RC, Wang J, Wolf RM, Wu X, York DM, Kollman PA. AMBER, version 14. San Francisco, CA: University of California; 2015

[31] Maestro, version 9.0. Portland, OR: Schrödinger Inc.; 2009

[32] Macromodel, version 9.7. Portland, OR: Schrödinger Inc.; 2009

[33] Morris GM, Goodsell DS, Halliday RS, Huey R, Hart WE, Belew RK, Olson AJ. Automated docking using a lamarckian genetic algorithm and an empirical binding free energy function. J Comput Chem 1998; 19: 1639–1662

[34] Morris GM, Huey R, Lindstrom W, Sanner MF, Belew RK, Goodsell DS, Olson AJ. AutoDock4 and AutoDockTools4: automated docking with selective receptor flexibility. J Comput Chem 2009; 30: 2785–2791